Proteomic and Functional Analyses Reveal a Mitochondrial Dysfunction in P301L Tau Transgenic Mice*

teins. Consistent with these findings, P301L tau mice exhibited mitochondrial functional defects together with reduced electron transport chain complex I activity. Aged P301L tau mice showed impaired mitochondrial respiration, reduced complex V activity, and higher levels of ROS than WT controls. Furthermore, modified lipid peroxidation and increased antioxidant enzyme activities were detected in aged homozygous mice. We also found an increased vulnerability of P301L tau mitochondria to Aβ insult, suggesting a synergistic action of tau and Aβ pathology on the mitochondria. Corroborating the P301L tau mouse mitochondrial deficits, we could demonstrate a reduction in complex V levels in human P301L FTDP-17 brains, implying a potential mitochondrial dysfunction in human patients afflicted with this neurodegenerative disorder.

EXPERIMENTAL PROCEDURES

– The transgenic mice used in the present study express the human pathogenic mutation P301L of tau together with the longest human brain tau isoform (htau40) under control of the neuron-specific mThy1.2 promoter (7). This isoform contains exons 2 and 3 as well as four microtubule-binding repeats (2^+3^+4R, human tau40). Pronuclear injections were done into C57Bl/6 $\times$ DBA/2 F_2 oocytes to obtain founder animals that were back-crossed with C57Bl/6 mice to establish transgenic lines. In addition, homozygous P301L tau mice were obtained and confirmed by TaqMan real-time quantitative PCR (data not shown).

Different age sets of mice were used for different experimental procedures corresponding to various stages in the development of tau pathology. P301L tau mice show tau hyperphosphorylation already at 3 months (7). NFT formation starts at 6 months of age (20). We used 8.5–10-month-old mice for the proteomics analysis to study the consequences of tau pathology at the beginning of NFT formation without the influence of aging. At a similar age (. . 12 months old), mitochondrial membrane potential and complex I and IV activity were determined. ATP levels, mitochondrial respiration, and ROS levels were analyzed in mice at 12 and 24 months of age. 24-month-old mice are expected to bear the highest levels of tau pathology. 18-month-old mice were used to determine mitochondrial numbers in neurites. This intermediate age allows us to see the full effect of tau pathology on mitochondrial transport without pronounced aging effects such as those seen in 24-month-

say Kit, sodium nitroprusside, rotenone, thenoyltrifluoroacetone, antimycin, sodium azide (NaN_3), and oligomycin were obtained from Sigma-Aldrich. $A\beta_{1-42}$ (Bachem, Weil am Rhein, Germany) was dissolved in Tris-buffered saline, pH 7.4, at a concentration of 1 mM and stored at −20 °C. The stock solution was diluted in Tris-buffered saline to the desired concentrations and incubated at 37 °C for 24 h to obtain aged, aggregated preparations of $A\beta_{1-42}$. All aqueous solutions were prepared with deionized and filtered water (Millipore).

B – Mice (8 pairs of 12-month-old and 8 pairs of 24-month-old hemizygous P301L tau and WT control mice) were sacrificed by decapitation, and brains were quickly dissected on ice (described in Ref. 22, with modification). After removing the cerebellum, one hemisphere (the other hemisphere was directly used for preparation of isolated mitochondria) was minced into 1 ml of medium I (138 mM NaCl, 5.4 mM KCl, 0.17 mM Na_2HPO_4, 0.22 mM K_2PO_4, 5.5 mM glucose, and 582033381.5139251(of.51bed)-3.513.528620.773[(Mice)-31scalpe1(m45133.15851furne)-39851Rheincir

and 2 mM EDTA, pH 7.0. State 4 respiration was measured after adding 40 μl of malate/glutamate (240/280 mM; assay concentration, 4.8/5.6 mM). Then, 10 μl of ADP (100 mM; assay concentration, 0.5 mM) were added to measure state 3 respiration. After determining coupled respiration, 1 μl of carbonyl cyanide ,-trifluoromethoxyphenylhydrazone (FCCP) (0.1 mM

method using the Lipid Peroxidation Assay Kit (Calbiochem) (31). The colorimetric reaction is a condensation of the aldehyde with 1-methyl-2-phenylindole, yielding a chromophore with an absorption maximum at 586 nm. Basal levels of MDA were assayed after incubation of samples for 30 min at 37 °C, and stimulated MDA levels were determined under the same conditions in the presence of 50 μM $FeCl_3$ in the sample homogenate.

C , ; D A – Cu,Zn-SOD (EC 1.15.1.1) activity was measured with the Superoxide Dismutase Assay Kit (Calbiochem) (32). To remove interfering substances and rule out Mn-SOD activity, Cu,Zn-SOD enzyme activity was assayed after an extraction procedure with chloroform and ethanol according to the supplier's manual. SOD activity was calculated based on the $_s/_c$ ratio of the auto-oxidation rates of the chromophore BXT-01050 measured at 37 °C in the presence ($_s$) and absence ($_c$) of sample. The chromophore was measured in a Genesys 5 photometer (Spectronic Instruments, Rochester, NY) at 525 nm. 1 Cu,Zn-SOD activity unit is defined as the activity that doubles the auto-oxidation background ($_s/_c = 2$).

B B A – Glutathione peroxidase (cytosolic glutathione peroxidase, EC 1.11.1.9) activity was measured using the Cellular Glutathione Peroxidase Assay Kit (Calbiochem) (33) and -butylhydroperoxide as substrate. This reaction is based on the enzymatic reduction of hydroperoxide by glutathione peroxidase under consumption of reduced glutathione, which is restored from oxidized glutathione in a coupled enzymatic reaction by glutathione reductase (GR). GR reduces oxidized glutathione to reduced glutathione under consumption of NADPH as reducing equivalents. The decrease in absorbance at 340 nm due to NADPH consumption was measured in a Victor2 multiplate reader using a 355-nm filter with 40 nm bandpass. 1 unit of glutathione peroxidase is defined as the activity that converts 2 μmol reduced glutathione/min at 25 °C.

A – The GR (EC 1.8.1.7.) activity was determined using the Glutathione Reductase Assay Kit (Calbiochem) (34). The enzymatic activity was assayed photometrically by measuring NADPH consumption during the enzymatic reaction. In the presence of oxidized glutathione and NADPH, GR reduces oxidized glutathione and oxidizes NADPH to yield NADP, resulting in a decrease of absorbance at 340 nm, which was measured in a Victor2 plate reader. 1 unit of GR is defined as the activity that reduces 1 μmol oxidized glutathione (corresponding to 1 μmol NADPH)/min at 25 °C.

; *A* – Data are represented as means ± S.E. For statistical comparison, Student's

either metabolism and mitochondrial respiration, oxidative stress, or synapse function. In the first category, we identified one spot as the 30-kDa subunit of NADH-ubiquinone oxidoreductase (electron transport chain complex I) and two spots as the ATP synthase D chain (complex V). All three spots were down-regulated as well as the metabolism-related spots, triosephosphate isomerase, a glycolytic enzyme, and the cytoplasmic malate dehydrogenase involved in the malate-aspartate shuttle providing a metabolic coordination between cytosol and mitochondria. In contrast, a spot identified as inorganic pyrophosphatase was up-regulated. Associated with oxidative stress, spots representing the antioxidant enzymes peroxiredoxin 6, perioredoxin 3 (thioredoxin-dependent peroxide reductase), glutathione ▲transferase (GST) P2 and Mu1, and phospholipid hydroperoxide glutathione peroxidase were all down-regulated. In the last functional category, we found up-regulated spots related to synaptic function, such as the synaptic vesicle-associated proteins synapsin I, CDCrel-1, and septin 11, the axonal growth-related protein dihydropyrimidinase-related protein (DRP)-2, and another member of the dihydropyrimidinase family, DRP-3. Further differentially regulated spots (Table I) included stathmin, a microtubule-destabilizing protein; MSTI1, the murine homologue of hop (HSP70/HSP90 organizing protein); and growth factor receptor-bound protein 2 (GRB2), an adapter protein in signaling pathways. Therefore, P301L tau expression results in distinct modifications of the brain pro-

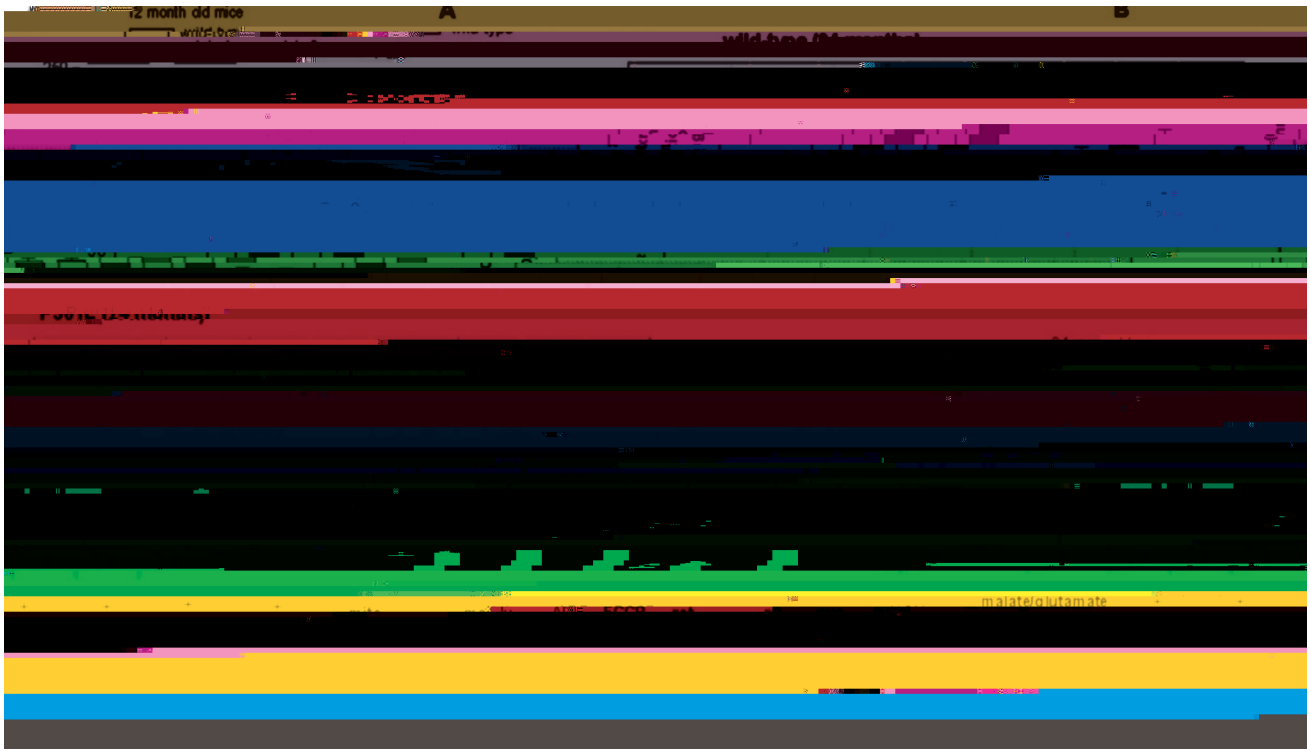

FIG. 4. **Oxygen electrode reveals a reduction of O_2 consumption of P301L tau mitochondria during aging.** *A*, representative diagrams of measurement of oxygen (O_2) consumption in mitochondria from a 24-month-old WT control (, ,) and an age-matched P301L tau mouse (, ,) demonstrating a decrease in the total O_2 concentration with time. O_2 flux and consumption by mitochondria (/) was measured after addition of different agents (marked by): malate/glutamate (/ / ; state 4), ADP (state 3), FCCP, rotenone (

spots identified as the ATP synthase D chain, we looked at complex V levels in human FTDP-17 patient brains carrying the P301L tau mutation. Four P301L FTDP-17 brain and two control brain homogenates were examined by Western blot (Fig. 2*A*). We used the mitochondrial protein marker porin to control for variations in mitochondrial amounts. Normalization of complex V levels with porin levels showed a significant decrease in complex V levels in all P301L brain samples compared with control brains (Fig. 2*B*). Similar control complex V/porin percentages were found in three other control brain samples (data not shown). On average, we measured a 62.3% reduction of complex V levels in P301L FTDP-17 brains compared with control brains. The decreased levels of complex V in human P301L FTDP-17 brains confirm the proteomics observation made in the P301L tau transgenic mice and suggest that the P301L mutant tau pathology potentially causes a specific mitochondrial dysfunction in humans as well as in mice.

301 , , – We examined the metabolic capacity and function of cerebral mitochondria from P301L tau transgenic mice. Consistent with the down-regulation of subunits of mitochondrial electron transport chain complexes I and V, treatment with specific complex inhibitors showed a general reduction in mitochondrial depolarization of P301L tau brain cells compared with WT and specifically showed a significantly reduced depolarization after inhibition of complexes I and V (Fig. 3*A*). Using a direct measurement of complex I activity, we observed a significant reduction of NADH-ubiquinone oxidoreductase (NADH:DBQ) activity in mitochondria of 12-month-old P301L tau mice (Fig. 3*B*), whereas NADH:HAR activity (Fig. 3*C*) was not different, indicating that complex I content is similar in P301L tau and WT control mice. Thus, P301L tau mitochondria present a functional defect of complex I activity with a reduction of 30.75% as revealed after normalization of complex I activity with complex I content (Fig. 3*D*). In contrast, complex IV showed no differences in the cytochrome, oxidase activity between WT and P301L tau transgenic mice (Fig. 3).

In addition, we determined the state 3 and state 4 respiration using substrates for complex I (glutamate/malate) (Fig. 4, *A* and *B*). State 3 respiration measures the capacity of mitochondria to metabolize oxygen and the selected substrate in the presence of a limited quantity of ADP, which is a substrate for the ATP synthase (complex V). State 4 respiration measures respiration when all ADP is exhausted, and it is associated with proton leakage across the inner mitochondrial membrane. Therefore, it represents a "basal-coupled" rate of respiration. Whereas state 3 and state 4 respiration remained unchanged with complex I substrates in 12-month-old P301L tau mice (Fig. 4*B*, , ,), a significantly reduced state 3 respiration could be observed in 24-month-old P301L tau mice (Fig. 4, *A* and *B*, , ,), leading to a markedly reduced respiratory control ratio compared with age-matched WT mice (Fig. 5*A*). The respiratory control ratio provides a measure for the efficiency of coupling of the mitochondrial respiratory chain,

indicating that the relative efficiency of metabolic coupling of the electron chain complexes is impaired during aging in P301L tau mice. In addition, after uncoupling with FCCP, the respiratory rate in the absence of a proton gradient was significantly diminished in 24-month-old P301L tau mice (Fig. 4*B*,), indicating a reduced maximum capacity of the electron transport chain. After complete inhibition of complex I with rotenone, succinate was added as a substrate for complex II. No difference in respiratory rate could be observed between transgenic and WT mice, showing that complex II is not impaired by P301L tau. In accordance with the respiratory control ratio, ATP levels of cerebral cells were unchanged in 12-month-old P301L tau transgenic mice but significantly reduced with aging (Fig. 5*B*). Together, these results suggest that P301L tau mice exhibit an initial defect in mitochondrial function with reduced complex I activity, which, with age, is translated into a mitochondrial respiration deficiency with diminished ATP synthesis corresponding to reduced complex V activity.

– Evaluation of the number of mitochondria in cerebral brain cells revealed no difference between P301L tau and WT mice either in the cerebrum (Fig. 6*A*) or in the cerebellum (data not shown). In addition, co-immunostaining of mitochondria and microtubules and subsequent counting of the mitochondria in proximal and distal parts of neurites in the CA1 region of the hippocampus also showed no variation between P301L tau and WT mice (Fig. 6*B*). These data suggest that mitochondrial dysfunction is not associated with reduced mitochondrial numbers or significant changes in transport of mitochondria along neurites.

301 , – In P301L tau mice, these mitochondrial defects are associated with increased ROS formation because both staining with DHE for detection of superoxide anions and staining with H_2DCF-DA for detection of cytosolic peroxides were increased (Fig. 7, *A* and *B*). Increased ROS levels could be detected already in 12-month-old P301L tau mice but were more pronounced and statistically significant in 24-month-old mice, correlating with the age-specific increase in tau pathology. As a measure of free radical damage to critical cellular components, levels of MDA as lipid peroxidation end product were determined. Despite increased ROS levels, basal levels of MDA were decreased in 24-month-old hemizygous P301L tau mice and more pronounced in homozygous mice, indicating that ROS levels are met by adequate antioxidant defenses in these mice (Fig. 7*C*). However, upon stimulation with ferric iron, increased MDA levels were formed in P301L tau mice (Fig. 7*D*). This effect was already observed in 12-month-old mice but was more pronounced and statistically significant in 24-month-old homozygous mice. Furthermore, basal and stimulated MDA levels remained unchanged in the cerebellum of 24-month-old hemi- and homozygous P301L tau and WT mice (data not shown). Because P301L tau is expressed at very low levels in the cerebellum (7), we can conclude that modifications in lipid peroxidation are specifically caused by the presence of the P301L tau protein. Hence, the presence of mutant tau impairs antioxidant defense under conditions of increased oxidative stress.

As a direct measure of antioxidant defense, activities of antioxidant enzymes were determined. Although no significant changes were observed in 12-month-old mice, 24-month-old homozygous P301L tau mice displayed increased activities of Cu,Zn-SOD and GR (Fig. 8, and), whereas the activity of glutathione peroxidase was not significantly increased (Fig. 8,

damao8 unao8 baso8condit,nao8

reports using positron emission tomography revealed reduced glucose metabolism in AD and frontotemporal dementia brains (12, 13, 47–49). Notably, high levels of phosphorylated tau have been linked to glucose hypometabolism in mild cognitively impaired patients (50).

Together, this evidence supports a role of tau pathology in mitochondrial and metabolic dysfunction. However, it remains unclear how tau accumulation mediates these changes. Overexpression of WT tau in cell culture caused impairment of plus end-directed transport, resulting in a reduction of mitochondria levels in the neurites (51). Although we cannot exclude the possibility of this occurring in the P301L tau mice, the number of mitochondria in neurites counted in proximity or distally to the cell body did not vary significantly compared with WT numbers. Furthermore, the total amount of mitochondria remained unchanged as measured in brain cells of transgenic compared with control mice. This suggests that either P301L tau induces a different pathological mechanism than overexpressed WT tau or that tau action on mitochondria transport in cell culture cannot be extrapolated over to the mouse model. Consistent with our findings, similar numbers of mitochondria were reported in NFT-bearing and non-NFT-bearing cells in AD (52). Alternatively, tau accumulation could have direct repercussions on the mitochondria because the accumulation of increasingly insoluble ATP synthase α-chain together with NFTs has been shown in AD brains, whereas detergent soluble levels were reduced (53). Overall, it is important to note that the mitochondrial pathology in the P301L tau mice observed in this study is unlikely to be a direct consequence of tau hyperphosphorylation. Indeed, the transgene levels of expression in these mice are relatively low (7), and depletion of ATP solely due to tau hyperphosphorylation would be improbable.

We furthermore demonstrate that accumulation of P301L tau causes significant modifications in the oxidative state of the brain. ROS measurements revealed increased levels of cytosolic H_2O_2 and superoxide anion radicals in 2-year-old P301L tau mice. These increased ROS levels may be a direct consequence of reduced complex I activity in P301L tau mice because inhibition of complex I can lead to increased superoxide formation (54). The increased activity of Cu,Zn-SOD measured in P301L tau mice should ameliorate the accumulation of superoxide but also gives risegivesT*[c

brains can protect against lipid peroxidation (55). Furthermore, SOD can prevent lipid peroxidation both β and β (56–60). Similarly, increased GR activity in P301L tau mice may protect against accumulation of MDA by increasing levels of the antioxidant reduced glutathione. In several experimental models, increased levels of reduced glutathione were associated with lower levels of lipid peroxidation products and vice versa (61, 62). Upon β stimulation, however, higher levels of MDA were formed in homozygous P301L tau brain homogenates. Obviously, the increased activities of Cu,Zn-SOD and GR were not sufficiently protective under these conditions.

antioxidant defense mechanisms in response to increased ROS levels in this mouse model. Because mitochondrial dysfunction appears prior to oxidative stress, this suggests that it is probably the initiating factor. However, we can speculate that both mitochondrial dysfunction and oxidative stress act in synergy, creating a vicious cycle. Indeed, increases in ROS and antioxidant enzyme dysfunction could affect the integrity of the mitochondria and, in particular, the electron transport chain (35). Furthermore, glutathionylation of complex I in oxidative conditions leads to increased superoxide production (71). Another possible consequence of higher oxidative stress levels could be an acceleration of tau pathology (72, 73). Moreover, tau can be readily oxidized by H_2O_2 to form disulfide-linked species that manifest reduced propensity to promote microtubule assembly (74). Oxidized tau then becomes a substrate of the thioredoxin reductase and glutathione/glutaredoxin reductase systems (74, 75). Thereby, we can speculate that the accumulation of oxidized P301L tau might overload these antioxidant regenerating systems, causing further oxidative stress.

Results from our proteomic study further suggest a potential synaptic dysfunction because we found an up-regulation of a series of synapse-related proteins. The identified DRP-2 is known to promote axonal growth by interaction with the tubulin heterodimer and has also been shown to induce neurite formation (76, 77). Synapsin I is thought to regulate the reserve pool of synaptic vesicles (78). The septin member CDCrel-1 is found mainly in inhibitory presynaptic terminals and inhibits exocytosis (79, 80). Interestingly, both DRP-2 and septin associate with NFTs in AD (81, 82). Therefore, in response to tau pathology, the transgenic mouse neurons may be attempting a compensatory mechanism by increasing synaptic vesicle control proteins and potentially aberrant synaptic sprouting. Indeed, although advanced stages of AD are associated with synaptic loss, an initial increase in synaptic protein levels in AD brains was observed that was correlated with the appearance of the tau pathology but not with Aβ plaques (83). On the contrary, a decrease of synaptic proteins occurred only after the appearance of the full spectrum of tau and Aβ pathology. Although it is uncertain exactly how tau mechanistically affects synapses, we can postulate that the mutant tau acts either by modifying microtubule stability and axonal transport or by

18. Sayre, L. M., Zelasko, D. A., Harris, P. L., Perry, G., Salomon, R. G., and Smith, M. A. (1997) . / . **68,** 2092–2097
19. Marcus, D. L., Thomas, C., Rodriguez, C., Simberkoff, K., Tsai, J. S., Strafaci, J. A., and Freedman, M. L. (1998) , . **150,** 40–44
20. Gotz, J., Chen, F., van Dorpe, J., and Nitsch, R. M. (2001) **293,** 1491–1495
21. Rabilloud, T., Carpentier, G., and Tarroux, P. (1988) , **9,** 288–291
22. Stoll, L., Schubert, T., and Muller, W. E. (1992) . **13,** 39–44
23. Lowry, O. H., Rosebrough, N. J., Farr, A. L., and Randall, R. J. (1951) . / . **193,** 265–275
24. Krohn, A. J., Wahlbrink, T., and Prehn, J. H. (1999) . . **19,** 7394–7404
25. Collins, T. J., Berridge, M. J., Lipp, P., and Bootman, M. D. (2002) . **21,** 1616–1627
26. Crouch, S. P., Kozlowski, R., Slater, K. J., and Fletcher, J. (1993) . / / . **160,** 81–88
27. Kenney, A. M., and Kocsis, J. D. (1998) . . **18,** 1318–1328
28. Budd, S. L., Castilho, R. F., and Nicholls, D. G. (1997) . **415,** 21–24
29. Djafarzadeh, R., Kerscher, S., Zwicker, K., Radermacher, M., Lindahl, M., Schagger, H., and Brandt, U. (2000) / . . **1459,** 230–238
30. Rasmussen, U. F., and Rasmussen, H. N. (2000) . / . **208,** 37–44
31. Esterbauer, H., and Cheeseman, K. H. (1990) . / . **186,** 407–421
32. Nebot, C., Moutet, M., Huet, P., Xu, J. Z., Yadan, J. C., and Chaudiere, J. (1993) . / . **214,** 442–451
33. Paglia, D. E., and Valentine, W. N. (1967) . . **70,** 158–169
34. Mizuno, Y., and Ohta, K. (1986) . / . **46,** 1344–1352
35. Keil, U., Bonert, A., Marques, C. A., Scherping, I., Weyermann, J., Strosznajder, J. B., Muller-Spahn, F., Haass, C., Czech, C., Pradier, L., Muller, W. E., and Eckert, A. (2004) . / . **279,** 50310–50320
36. Spillantini, M. G., Van Swieten, J. C., and Goedert, M. (2000) , **2,** 193–205
37. Pennanen, L., Welzl, H., D'Adamo, P., Nitsch, R. M., and Gotz, J. (2004) . **15,** 500–509
38. Schonberger, S. J., Edgar, P. F., Kydd, R., Faull, R. L., and Cooper, G. J. (2001) , **1,** 1519–1528
39. Butterfield, D. A., Boyd-Kimball, D., and Castegna, A. (2003) . / . **86,** 1313–1327
40. Molloy, M. P., Herbert, B. R., Walsh, B. J., Tyler, M. I., Traini, M., Sanchez, J. C., Hochstrasser, D. F., Williams, K. L., and Gooley, A. A. (1998) , **19,** 837–844
41. Sims, N. R., Finegan, J. M., Blass, J. P., Bowen, D. M., and Neary, D. (1987) . **436,** 30–38
42. Aksenov, M. Y., Tucker, H. M., Nair, P., Aksenova, M. V., Butterfield, D. A., Estus, S., and Markesbery, W. R. (1999) . / . . **24,** 767–774
43. Li, Y. J., Oliveira, S. A., Xu, P., Martin, E. R., Stenger, J. E., Scherzer, C. R., Hauser, M. A., Scott, W. K., Small, G. W., Nance, M. A., Watts, R. L., Hubble, J. P., Koller, W. C., Pahwa, R., Stern, M. B., Hiner, B. C., Jankovic, J., Goetz, C. G., Mastaglia, F., Middleton, L. T., Roses, A. D., Saunders, A. M., Schmechel, D. E., Gullans, S. R., Haines, J. L., Gilbert, J. R., Vance, J. M., Pericak-Vance, M. A., Hulette, C., and Welsh-Bohmer, K. A. (2003) / . . **12,** 3259–3267
44. Bowling, A. C., Mutisya, E. M., Walker, L. C., Price, D. L., Cork, L. C., and Beal, M. F. (1993) . / . **60,** 1964–1967
45. Orosz, F., Wagner, G., Liliom, K., Kovacs, J., Baroti, K., Horanyi, M., Farkas, T., Hollan, S., and Ovadi, J. (2000) . . . **97,** 1026–1031
46. Castegna, A., Thongboonkerd, V., Klein, J. B., Lynn, B., Markesbery, W. R., and Butterfield, D. A. (2003) . / . **85,** 1394–1401
47. Mielke, R., Schroder, R., Fink, G. R., Kessler, J., Herholz, K., and Heiss, W. D. (1996) . **91,** 174–179
48. Diehl, J., Grimmer, T., Drzezga, A., Riemenschneider, M., Forstl, H., and Kurz, A. (2004) . **25,** 1051–1056
49. Grimmer, T., Diehl, J., Drzezga, A., Forstl, H., and Kurz, A. (2004) / . . **18,** 32–36
50. Fellgiebel, A., Siessmeier, T., Scheurich, A., Winterer, G., Bartenstein, P., Schmidt, L. G., and Muller, M. J. (2004) . **56,** 279–283
51. Ebneth, A., Godemann, R., Stamer, K., Illenberger, S., Trinczek, B., and Mandelkow, E. (1998) . / . **143,** 777–794
52. Sumpter, P. Q., Mann, D. M., Davies, C. A., Yates, P. O., Snowden, J. S., and Neary, D. (1986) , . . **12,** 305–319